Rui Filipe Cantarino Valente de Almeida

Master of Science

Development of a Tomographic Atmospheric Monitoring System based on Differential Optical Absorption Spectroscopy

Thesis plan submitted in partial fulfillment
of the requirements for the degree of

Doctor of Philosophy in
Biomedical Engineering

Adviser: Pedro Vieira, Auxiliar Professor,
NOVA University of Lisbon

FACULDADE DE
CIÊNCIAS E TECNOLOGIA
UNIVERSIDADE NOVA DE LISBOA

September, 2019

Contents

List of Figures

List of Tables

Acronyms

AP Air Pollution

CT Computed Tomography

DOAS Differential Optical Absorption Spectroscopy

EPA Environmental Protection Agency (United States)

FBP Filtered BackProjection

FFF Forest Fire Finder

FST Fourier Slice Theorem

FT Fourier Transform

ICE Internal Combustion Engine

IFT Inverse Fourier Transform

ML Machine Learning

PM Particulate Matter

ROI Region Of Interest

RQ Research Question

SLR Systematic Literature Review

VOC Volatile Organic Compound

WHO World Health Organization

*

Chapter 1

Background and Motivation

1.1 Context

The idea behind this thesis was born in 2015, at NGNS-IS (a Portuguese tech startup). At the time, the company's flagship product was the Forest Fire Finder (FFF). The FFF was a forest fire detection system, capable of mostly autonomous and automatic operation. The system was the first application of Differential Optical Absorption Spectroscopy DOAS for fire detection, and for that it was patented in 2007 (see [24, 25]). The FFF is a remote sensing device that scans the horizon for the presence of a smoke column, sequentially performing a chemical analysis of each azimuth, using the Sun as a light source for its spectroscopic operations [23].

The FFF was deployed in several "habitats", both nationally (Parque Nacional da Peneda-Gerês and Ourém) and internationally (Spain and Brazil). One of the company's clients at the time was interested in a pollution monitoring solution, and asked if the spectroscopic system would be capable of performing such a task. The challenge resonated through the company's structure and the idea that created this thesis was born. The team then started reading about the concept of Air Pollution AP and how both populations and entities were concerned about it. It became clear that, while there were already several methods to measure AP, there was a clear market drive for the development of a system that could leverage the large area capabilities of a DOAS device while being able to provide a more spatially resolved "picture" of the atmospheric status. With this in mind, the company managed to have the investigation financed through a PT2020 funding opportunity. This achievement was a clear validation of the project's goals and of the need there was for a system with the proposed capabilities. It was, however, not enough. FFF was a very good starting point, but there was still a lot of continuous research work needed before any of the goals that had been set were achieved. This led to the publication of this PhD project, in a tripartite consortium between FCT-NOVA, NGNS-IS and the Portuguese Foundation for Science and Technology. Its main goal was to develop an atmospheric monitoring system prototype that would be able to spectroscopically map pollutant concentrations

in a two-dimensional way.

1.2 The Problem

The first step in tackling the development of the proposed system was to understand the problem it should be dealing with. Air Pollution (AP) is one of the most present concerns of people around the industrialized modern world. In Europe, it is perceived to be the second most important threat to the environment. The first is climate change, which is great part caused by AP. Scientists in many countries have established it as a major cause for premature death, disease onset and hospital visits for some decades now. Regulatory bodies of many countries have been gathered to put some legislative pressure on industries and on society itself, in order to produce a decrease in the amount of Air Pollution to which people are exposed. These policies and measures have had a dramatic influence in air quality, which is very significantly improved throughout the years. In spite of this, official reports continue to highlight the importance of keeping a vigilant eye towards AP proliferation and its possible undiscovered health effects. A better introduction to the subject of AP is produced in Section 2.1.

Our spectacular progress as a species in the last few centuries has had some unforeseen adverse consequences. Mitigating them is not only a responsibility, but also a necessity. In some regards, as is the AP case, this mitigation is only achievable with intelligent and effective action. This of course demands that we understand, trace and measure it in as many ways as possible. This project aimed to create just that: another way in which to measure and map the behavior of certain pollutants.

1.3 Objectives

From the beginning of the project, the main objective has always been to design and develop a miniaturized spectroscopic environmental analysis device. The system would have to be small and portable enough to adapt to a drone, but should be able to function if adapted to any other surface, such as a car or even a fixed station. With time, however, the goal changed somewhat. The miniaturization and drone-adaptation were kept, but there was now the need to be able to map the pollutant concentration along a geographic region through the use of tomographic reconstruction algorithms. This meant that, while the device itself would be perfectly capable of operating without a drone, the tomographic capability would be lost, unless a prohibitively large number of spectroscopic systems were deployed in that region.

The concept evolved in such a way that the overarching goal of this thesis is now to theorize and design a two-dimensional mapping tool for trace atmospheric pollutants such as NO_x and SO_x, using passive DOAS as the measurement technique. In addition to this, it should be mentioned that the system must be small and portable; use tomographic reconstruction (and acquisition) algorithms to map the region; and that

it should use only one collection point (to reduce costs and instrumental complexity). From these objectives, the research questions, detailed in Section 2.2 were derived.

Chapter 2

Research Question

2.1 Problem Introduction

AP is a very important topic of discussion in the current days, with scientists and researchers around the globe being very well aware of the potential effects it can have on the health of individuals and populations across all ecosystems [17]. After climate change (one of the largest capital threats to life on Earth, perhaps just behind nuclear apocalypse), AP is the biggest environmental concern for Europeans, and Europe's single largest environmental health hazard [8]. It has also been established by many authors as a major cause of premature death, cardiopulmonary disease onset and hospital visits [7–9, 26].

The growing concerns about Air Pollution and its effects on human health and the world in general is an indication for the importance of measuring it correctly and with great detail. The diversity of its effects and the sheer number of variables that need to be considered establish the problem of AP as one that can only be effectively tackled if approached intelligently, highlighting the need for smart devices for the measuring and monitoring atmospheric pollutants.

At the moment, there are several solutions that can be implemented for measuring atmospheric pollution. However, these solutions are limited in their application to either large area coverage and small details (DOAS ground stations, satellite data) or very detailed information in a very localized and fixed way (in-situ electrochemical sensors). To the best of our knowledge, there are no available systems that can monitor and map pollutant concentration without requiring infrastructure installation and capable of performing at various altitudes.

The answer to this lack could be a highly mobile tomographic DOAS system, that could bridge the gap between the local monitoring capabilities of in-situ electrochemical sensors and large-area spectroscopic ground stations, while maintaining portability and flexibility.

2.2 Research Question

In Chapter 1, I have introduced the reasons which led NGNS-IS to pursue the development of an atmospheric monitoring system, and that what set it apart from other systems was the ability to spectroscopically map pollutants concentrations using tomographic methods, thus defining a primary objective for this thesis.

Two secondary objectives were born from the necessary initial research, which had a very heavy influence over the adopted methods:

- To use a tomographic approach for the mapping procedure;
- To ensure the designed system would be small and highly mobile;
- To use a single light collection point, minimizing material costs.

Taking all the above into account, we arrive at the main Research Question (RQ), presented in Table 2.1.

Table 2.1: Main research question.

RQ1	*How to design a miniaturized tomographic atmosphere monitoring system based on DOAS?*

This is the main research question. It gave rise to four other more detailed research questions. These secondary questions allow a better delimitation of the work at hand and are important complements to RQ1. This questions are presented in Table 2.2

Table 2.2: Secondary research questions.

RQ1.1	*What would be the best strategy for the system to cover a small geographic region?*
RQ1.2	*What would be the necessary components for such a system?*
RQ1.3	*How will the system acquire the data?*
RQ1.4	*What should the tomographic reconstruction look like and how to perform it?*

2.3 Hypothesis and Approach

This work is based on the hypothesis that a system such as the one described in Chapter 1, which responds to the RQ in Table 2.1 and Table 2.2 can be achieved by careful selection of mathematical tomographic algorithms and instrumentation that is able to implement them correctly.

The first step in answering the entirety of the research questions should be to answer RQ1.1. In fact, it is not possible to make any other decision before this matter is settled. As with any technical problem, there are several ways to create a tomographic atmospheric monitoring tool. However, each and every one of them implies some kind of compromise, which determines the system's capabilities and requirements. Will the system use retro-reflection? Shall it move during the measurement? These are the kind of questions that determine the whole project.

When the measurement strategy is determined, one could start picking parts and components. However, a better first approach would be designing a software simulation. This simulator must include all major system features, so that it correctly mimics reality and is therefore able to mathematically validate the acquisition and reconstruction approach. The results obtained from the simulation will then dictate mechanical and control requirements.

One other aspect that needs addressing is the optical section. As mentioned before, the system will be inspired in FFF's basic optical capabilities. However, the smoke detector was not conceived with spatial restrictions in mind. This important set of components will thus need redesigning, so that it is in line with the size objectives of the new system.

Chapter 3

Literature Review

In this chapter, I provide a literary review on the three most important subjects for the work of this thesis: AP, tomographic algorithms and DOAS tomography instrumentation.

3.1 Air pollution and pollutants

As stated in Section 2.2, the definition of AP is dependent on the context. Here, I will focus especially on the effects of pollutants on human health. Whether these effects are the most significant problems stemming from AP is debatable (climate change is mostly caused by anthropogenic production of greenhouse gases, which are pollutants) but for this system and its intended uses, health effects are definitely more prominent. Human health implications of a polluted atmosphere are documented in very numerous studies throughout the literature. In this document, I will only present a small number of representative reviews and reports.

In 2004, WHO published a report summarizing what was then the most recent information on health effects of air pollution over Europe. This review concluded that, even with all the regulations on AP put in place by the European authorities, its levels were still posed a considerable burden on health throughout Europe [26].

Although there are several hundred potentially harmful components already that have already been found in the atmosphere, this report addresses only PM, ground level Ozone and Nitrogen Dioxide. As many other studies had found, this Systematic Literature Review (SLR) identified several short-term and long-term exposure effects for the three pollutants. The study found that short-term exposure to all three substances were responsible for an increase in mortality and hospital admissions, and that both PM and O_3 increased the population's usage of medication. Long-term exposure to all three components have adverse pulmonary effects, but PM have many other negative effects. The most important of them a reduction in life expectancy, which the authors attribute to cardiopulmonary mortality and lung cancer.

Particulate Matter are described as airborne solid particles or droplets. These

particles vary in size, origin and composition, however, it is usual to classify them by size, since that is what governs particle deposition in the respiratory system. Urban PM are usually divided into three categories: coarse, fine and ultrafine. Convention dictates that coarse particles have an aerodynamic diameter of less that 10μm (PM_{10}), fine particles less than 2.5μm ($PM_{2.5}$). In this review, the authors stated that the role that ultrafine particles play in human health is still undetermined, but they noted that coarse and (especially) fine particles are highly correlated with an increase in mortality and the prevalence of respiratory syndromes [26].

Ground-level ozone is produced as a result of a chemical reaction between nitrous oxides and Volatile Organic Compounds (VOC), which can be emitted either by natural source or by human-related activities. O_3 is a powerful oxidant, and can easily accept electrons from other molecules. In the respiratory tract, this chemical destroys double bonds of the fatty acids in the surface of its lining. The process leads to the deposition of several substances like aldehydes and hydrogen peroxide, resulting in impaired cell function. Ozone is toxic at concentrations that occur in urban areas around the world. On a more ecological level, it has been established that O_3 is responsible for a decrease in the trees' capabilities to assimilate carbon, which can result in deforestation.

Nitrous Oxides originate from the use of Internal Combustion Engines (ICE) for energy production and especially movement. It is usually used as an indicator for the presence of heavy traffic. The compound acts in a more subtle way than Ozone, described above. It increases the risk of respiratory infections and can cause pulmonary edema. Moreover, it has an effect on the immunological system, impairing the ability of T-lymphocytes to address microbiological threats like viruses. Nitrous oxides are also known to affect weaker populations, like children and the elderly.

3.2 Tomographic algorithms and reconstruction techniques

3.2.1 Introduction

Tomography is the cross-sectional imaging of an object through the use of transmitted or reflected waves, captured by the object exposure to the waves from a set of known angles. It has many different applications in science, industry, and most prominently, medicine. Since the invention of the Computed Tomography (CT) machine in 1972, by Hounsfielf [11], tomographic imaging techniques have had a revolutionary impact, allowing doctors to see inside their patients, without having to subject them to more invasive procedures [15].

Mathematical basis for tomography were set by Johannes Radon in 1917. At the time, he postulated that it is possible to represent a function written in $\mathbb{R}$ in the space of straight lines, $\mathbb{L}$ through the function's line integrals. A line integral is an integral in which the function that is being integrated is evaluated along a curved path, a line.

In the tomographic case, these line integrals represent a measurement on a ray that traverses the Region Of Interest (ROI). Each set of line integrals, characterized by an incidence angle, is called a projection (see Figure 3.1). To perform a tomographic reconstruction, the machine must take many projections around the object. To the set of projections arranged in matrix form by detector and projection angle, we call sinogram. All reconstruction methods, analytical and iterative, revolve around going from reality to sinogram to image [3, 6, 12–15].

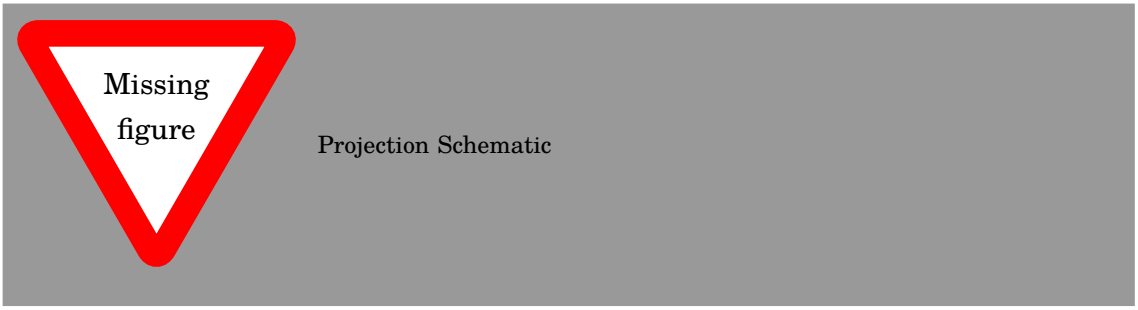

Figure 3.1: A schematic representation of a projection.

There are two broad algorithm families when it comes to tomographic reconstruction, regarding the physics of the problem. The problem can involve either non-diffracting sources (light travels in straight lines), such as the X-Rays in a conventional CT exam; or diffracting sources, such as micro-waves or ultrasound in more research-oriented applications. In this document, I will not address the latter family, since I will not be applying them in my work. In the next few paragraphs, I will discuss the first family of algorithms, and describe how an image can be reconstructed from an object's projections when the radiation source is non-diffracting.

Let's consider the case in which we deal with a single ray of solar light entering the atmosphere at a given point. Since the atmosphere contains numerous absorbents and comparable atmospheric effects, the ray changes from the point where it enters the atmosphere to the point at which it is measured by a detector. Total absorption will depend on the pollutant species, their cross-section and their concentration, since it obeys Lambert-Beer's law. Looking from another angle, this absorption is also the line integral that we will use to reconstruct our image. With DOAS, it is possible to measure several pollutants at the same time, but for simplicity (and since it is one of the most studied compounds in the field), let's consider that the single pollutant in our atmospheric mixture is NO_2.

3.2.2 Initial Considerations

The problem of tomographic reconstruction can be approached in a number of ways, depending mostly on the authors. In my literary search, I have found that Kak and Slaney [15] have certainly explained this problem in one of the clearer ways available.

Therefore, I shall base the rest of my presentation in their writings, and complement with other authors' notes wherever necessary.

Considering the coordinate system displayed in Figure 3.2. In this schematic, the object is represented by the function $f(x, y)$. The (θ, t) parameters can be used to define any line in this schematic. Line AB in particular can be written:

$$x \cdot \cos(\theta) + y \cdot \sin(\theta) = t \tag{3.1}$$

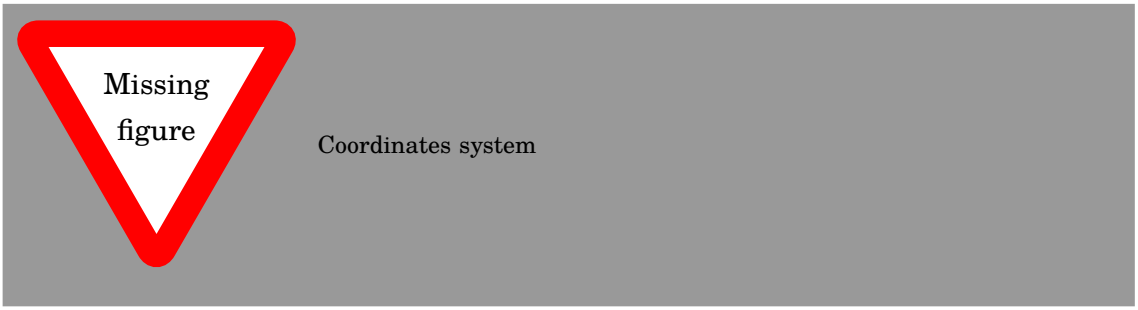

Figure 3.2: Schematic representation for coordinate setting.

And if we were to write a line integral along this line, it would look like Equation 3.2, the Radon transform of function $f(x, y)$:

$$P_\theta(t) = \int_{-\infty}^{\infty} f(x, y) \cdot \delta(x \cdot \cos(\theta) + y \cdot \sin(\theta) - t) dx dy \tag{3.2}$$

Where δ, the delta function, is defined in Equation 3.3.

$$\delta(\phi) = \begin{cases} 1, & \phi = 0 \\ 0, & otherwise \end{cases} \tag{3.3}$$

As I have mentioned previously, a projection is a set of line integrals such as $P_\theta(t)$. Geometry plays a very important role in how the integrals are written and solved for reconstruction. The simplest case is the one where the set is acquired in a row, describing what is called a parallel geometry. Another more complex case is when a single point source is used as origin for all rays, forming a fan. This is called a fanbeam array. There are other possible geometries, but they fall out of the scope of this work and will therefore not be addressed any further.

3.2.3 The Fourier Slice Theorem

The Fourier Slice Theorem (FST) is the most important component of the most important algorithm in tomographic inversion, the Filtered BackProjection algorithm (FBP). FST is based on the equality relation between the two-dimensional Fourier Transform (FT) of the object function and the one-dimensional FT of the object's projection at an

angle θ. Let's start by writing the 2D FT for the object function, Equation 3.4, and the 1D FT of projection P_θ, in Equation 3.5.

$$F(u,v) = \int_{-\infty}^{\infty}\int_{-\infty}^{\infty} f(x,y)\cdot \exp\left[-j2\pi(ux+vy)\right] dxdy \tag{3.4}$$

$$S_\theta(\omega) = \int_{-\infty}^{\infty} P_\theta \cdot \exp\left[-j2\pi\omega t\right] \tag{3.5}$$

For simplicity, let's consider the 2D FT at the line defined by $v = 0$ in the frequency domain. We rewrite the 2D FT integral as:

$$F(u,0) = \int_{-\infty}^{\infty}\int_{-\infty}^{\infty} f(x,y)\cdot \exp\left[-j2\pi\omega ux\right] dxdy \tag{3.6}$$

Notice that y is not present in the phase factor of the FT expression anymore, and this means we can rearrange the integral as:

$$F(u,0) = \int_{-\infty}^{\infty}\left[\int_{-\infty}^{\infty} \mathbf{f(x,y)dy}\right]\cdot \exp\left[-j2\pi\omega ux\right] dx \tag{3.7}$$

Now, the **bold** part of Equation 3.7 is similar to Equation 3.2. It is precisely that equation, considering $\theta = 0$ and a constant value of x, as in Equation 3.8.

$$P_{\theta=0}(x) = \int_{-\infty}^{\infty} f(x,y)dy \tag{3.8}$$

This in turn can be substituted in Equation 3.7, finally arriving at:

$$F(u,0) = \int_{-\infty}^{\infty} P_{\theta=0}(x)\cdot \exp\left[-j2\pi ux\right] dx \tag{3.9}$$

And this is the one-dimensional FT for the projection at angle $\theta = 0$. Finally, the enunciation of the Fourier Slice Theorem:

> ***The Fourier Transform of a parallel projection of an image*** $f(x,y)$ ***taken at angle*** θ ***gives a slice of the two-dimensional Fourier Transform,*** $F(u,v)$***, subtending an angle*** θ ***with the*** u***-axis (see Figure 3.3)***

3.2.4 The Filtered BackProjection Algorithm

3.2.4.1 The rationale for FBP

If one takes the FST into account, the idea behind the FBP seems to appear almost naturally. Say one has a single projection and its Fourier transform. From the FST, this projection is the same as the object's two-dimensional FT in a single line. A crude reconstruction of the original object would result if someone were to place this projection in its right place in the Fourier domain and then perform a two-dimensional IFT, while assuming every other projection to be 0. The result, in the image space, would be as if someone had smeared the object in the projections direction.

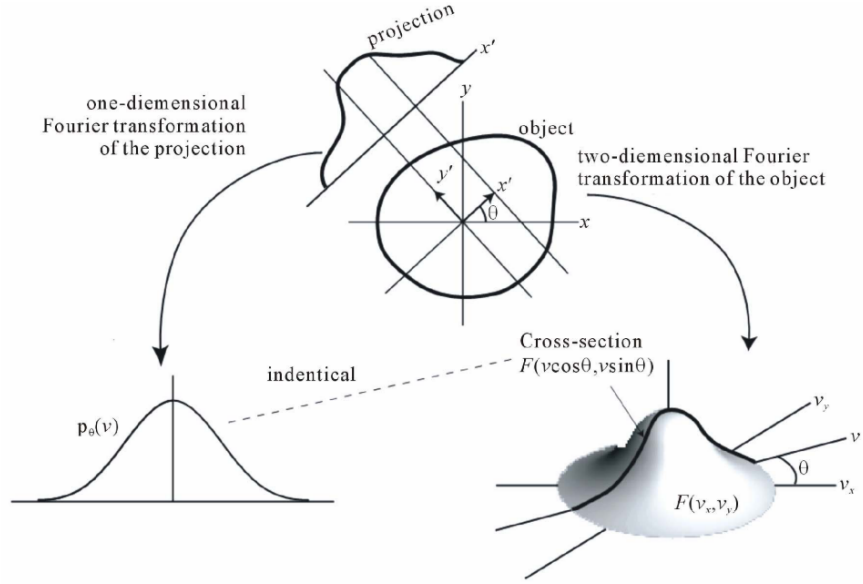

Figure 3.3: The FST, a schematic representation.

What is really needed for a correct reconstruction is to do this many times, with many projections. This brings a problem with the method: smearing the object in all directions will clearly produce a wrong *accumulation* in the center of the image, since every projection passes through the middle (remember we are still talking about parallel geometry projections) and are summed on top of each other, but on the outer edges, this does not occur. If one does not address this, the image intensity levels in the reconstructed image will be severely overestimated in the center and underestimated in the edges (due to normalization). The solution is conceptually easy: we multiply the Fourier transform by a weighting filter proportional to its frequency (ω) and that encompasses its relevance in the global scheme of projections. If there are K projections, then it is adequate for this value to be $\frac{2\pi|\omega|}{K}$. As an algorithm, FBP can be written as in Algorithm 1.

Algorithm 1 The Filtered BackProjection Algorithm

for all $\theta, \theta \in \{0..180, \frac{180}{K}\}$ **do**
  Measure projection $P_\theta(t)$;
  FT($P_\theta(t)$), rendering $S_\theta(\omega)$
  Multiply by $\frac{2\pi|\omega|}{K}$;
  Sum the IFT of the result in the image space.
end for

3.2.4.2 Fan Projections Reconstruction

Parallel projections, in which the object is scanned linearly from multiple directions, have the advantage of having a relatively simple reconstruction scheme. However, they

usually result in acquisition times which are in the order of minutes. A faster way of collecting the data is one where all radiation emanates from a single point-source, which rotates around the target object (as well as the detectors). There are two types of fan beam projections: equiangular and equally spaced. In this project, I have only worked with equiangular processes, so I will not include an explanation for equally spaced fan beam projections. The reader may find this well described (much better than I would be able to) in [15] and [14].

Consider Figure 3.4. If our projection data were acquired through a parallel ray geometry, we would be able to say that ray SA belonged to a projection $P_\theta(t)$, in which θ and t would be written:

$$\theta = \beta + \gamma \quad \text{and} \quad t = D \cdot \sin\gamma \tag{3.10}$$

In Equation 3.10, D is the distance between the source S and the origin O; γ is the angle of a ray within a fan and β is the angle that the source S makes with a reference axis.

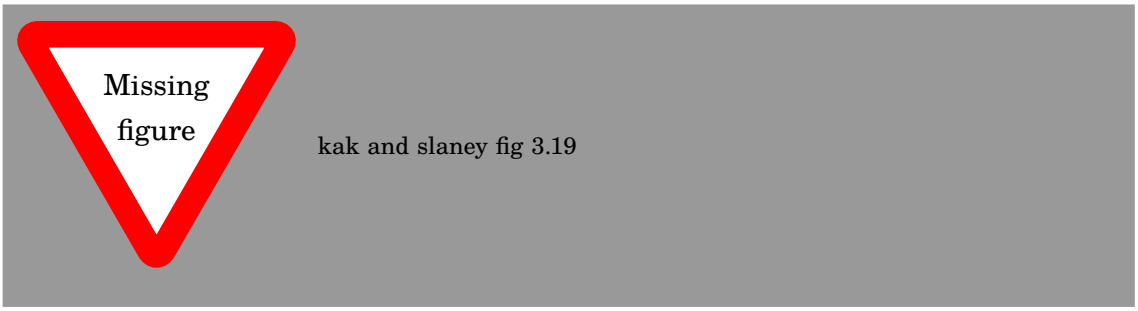

Figure 3.4: Schematic representation of an equiangular fan beam projection.

3.3 DOAS

Differential Optical Absorption Spectroscopy is a well-established absorption technique that is widely used in the field of atmospheric studies [20]. There are two main families of DOAS assemblies, with different goals and capabilities:

- Active systems, of which a simple illustration is presented in Fig. 3.5, are characterized by relying on an artificial light source for their measurements. A spectrometer at the end of the light path performs spectroscopic detection. Active DOAS techniques are very similar to traditional in-lab absorption spectroscopy techniques [20];

- Passive DOAS techniques, illustrated in Fig. 3.6, use natural light sources, such as the Sun and the moon, in their measurement process. An optical system is pointed in certain elevation and azimuth angles and sends the captured light

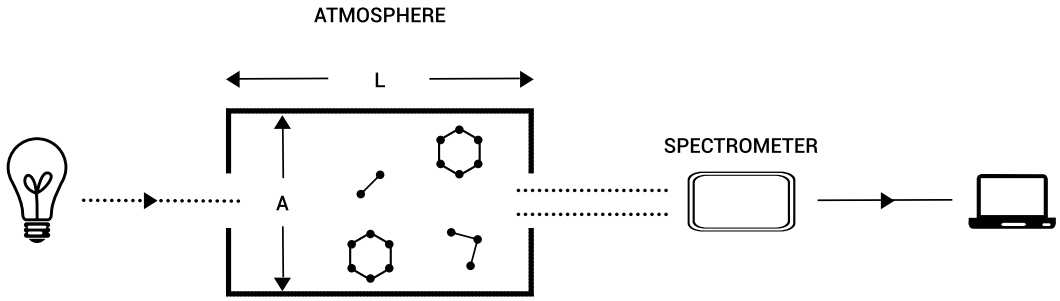

Figure 3.5: Active DOAS schematic.

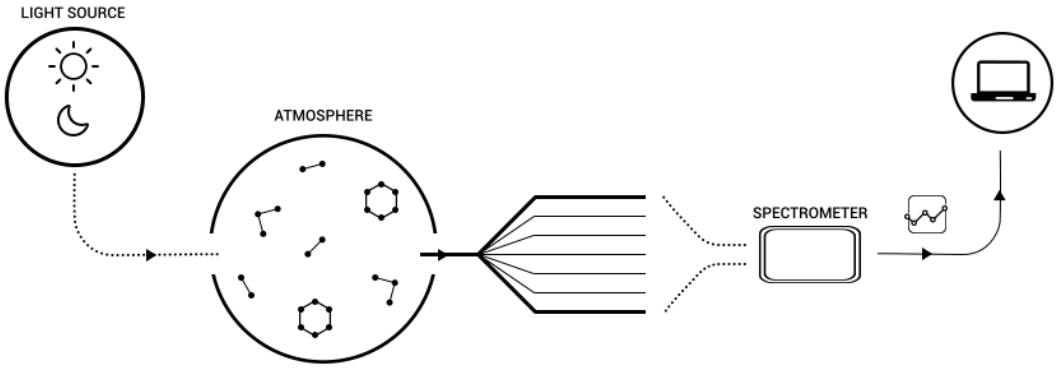

Figure 3.6: Passive DOAS schematic.

into a spectrometer, connected to a computer. The system returns the total value of the light absorption in its path [18, 20].

DOAS itself is based on Lambert–Beer's law, which can be written as [20]

$$I(\lambda) = I_0(\lambda) \cdot \exp(-\sigma(\lambda) \cdot c \cdot L) \ , \tag{3.11}$$

Where λ is the wavelength of the emitted light; $I(\lambda)$ is the light intensity as measured by the system; $I_0(\lambda)$ is the intensity of the light as emitted by the source; and $\sigma(\lambda)$ is the absorption cross section of absorber, which is wavelength dependent; c is the concentration of the absorber we want to measure.

This law allows the definition of optical thickness (τ) [20]:

$$\tau(\lambda) = \ln\left(\frac{I_0(\lambda)}{I(\lambda)}\right) = \sigma(\lambda) \cdot c \cdot L. \tag{3.12}$$

In a laboratory setting, Eq. (3.11) or (3.12) can be used to directly calculate an absorber's concentration, provided there is knowledge of its cross section. In the open atmosphere, however, absorption spectroscopy techniques are far more complex. On one hand, $I_0(\lambda)$ is not accessible since we measure from inside the medium we want to measure. On the other hand, there are several environmental and instrumental effects that influence measurement results. These effects include the following [20].

- Rayleigh scattering is due to small molecules present in the atmosphere and is heavily influenced by wavelength (hence the blue colour of the sky).
- Mie scattering is caused by particles and larger molecules suspended in the atmosphere and is not very dependent on the wavelength (hence the white colour of clouds).
- Instrumental and turbulence effects are the instrument's transmissivity and atmospheric turbulence in the optical path also limit light intensity.

In addition, we also have to take into account that, in the atmosphere, there are a number of trace gases that interfere with passing light.

Another aspect worth mentioning is that our device is never pointed directly at the light source (the Sun) but always processes light that has been scattered at some unknown point in the optical path. This means that the light that reaches our detector is only the scattered fraction of the sunlight, depending on the system's position and geometry, as well as wavelength.

The expansion of Lambert–Beer's equation to include all these effects results in Eq. (3.13).

$$\begin{aligned} I(\lambda) = I_0(\lambda) \cdot A(\lambda, \ldots) \cdot S(\lambda) \\ \cdot \exp\left[- \int \left[\Big(\sum_i \sigma_i(\lambda, s) \cdot c_i(s) \Big) + \epsilon_{\mathrm{M}}(\lambda, s) \right. \right. \\ \left. \left. + \epsilon_{\mathrm{R}}(\lambda, s) \right] \mathrm{d}s \right], \end{aligned} \tag{3.13}$$

where $A(\lambda, \ldots)$ is the fraction of scattered light that reaches the device, $S(\lambda)$ represents instrumental and turbulence effects, $\sigma_i(\lambda, s)$ is the absorption cross section of absorber i, c_i is the concentration of absorber i, $\epsilon_{\mathrm{R}}(\lambda)$ represents Rayleigh's extinction coefficient and $\epsilon_{\mathrm{M}}(\lambda)$ represents Mie's extinction coefficient.

The interest of this equation lies within the retrieval of c_i, a given absorber's concentration. Since the integral is taken along the total atmospheric path of the measured photons, and considering that their cross sections do not vary significantly in atmospheric conditions, it is possible to define the concept of slant column, which is of great importance [18].

$$\mathrm{SC}_i = \int c_i(s) \mathrm{d}s \tag{3.14}$$

This quantity, as Eq. (3.14) shows, equals the integral of an individual absorber's concentration along the atmospheric optical path of relevance.

Now, without knowledge of $I_0(\lambda)$, these equations cannot give us absolute concentration values. We can, however, use another scattered light spectrum as reference

in Eq. (3.12). Instead of absolute densities, this will yield relative changes in the atmosphere. We thus arrive at Eq. (3.15).

$$\begin{aligned}\ln\left(\frac{I_{\text{ref}}}{I}(\lambda)\right) = \ln\left(\frac{A_{\text{ref}}}{A}(\lambda,\ldots)\right) + \ln\left(\frac{S_{\text{ref}}}{S}(\lambda)\right) \\ + \sum_i(\sigma_i(\lambda)\cdot\Delta\text{SC}_i(\lambda)) + \Delta\tau_{\text{M}}(\lambda) \\ + \Delta\tau_{\text{R}}(\lambda),\end{aligned} \tag{3.15}$$

where ΔSC_i is the relative slant column of absorber i; $\Delta\tau_{\text{M}}$ is the relative Mie scattering term, integrated to its optical thickness; and $\Delta\tau_{\text{R}}$ is the relative Rayleigh scattering term, integrated to its optical thickness.

This is where the principle of DOAS is applied. Instrument features, scattering and other atmospheric effects have broad absorption spectral profiles, which vary slowly with wavelength. Several trace absorbers have narrow and rapidly varying spectral signatures in at least a small section of the spectrum. By using Eq. (3.16), we can separate these contributions [5].

$$\sigma(\lambda) = \sigma'(\lambda) + \sigma_0(\lambda) \tag{3.16}$$

Here, the broad part of the optical thickness ($\sigma_0(\lambda)$) can be separated from the narrow part ($\sigma'(\lambda)$ – differential) by approximating it by a low-order polynomial, resulting in Eq. (3.17).

$$\ln\left(\frac{I_{\text{ref}}}{I}(\lambda)\right) = \sum_{i=1}^{n}\sigma_i{}'(\lambda)\cdot\Delta\text{SC}_i + \sum_{j=0}^{m}a_j\cdot\lambda^j, \tag{3.17}$$

where $\sum_{i=1}^{n}\sigma_i{}'(\lambda)\cdot\Delta SC_i$ is the differential part (narrowband, rapidly varying with wavelength) and $\sum_{j=0}^{m}a_j\cdot\lambda^j$ is a low-order polynomial, used to remove the broadband spectral features resulting from atmospheric and instrumental phenomena.

In practice, the mathematical solving of Eq. (3.17) is not enough since it does not account for the Ring effect or the non-linearities that result from stray light and wavelength shift in measured and cross-section spectra.

The Ring effect is a consequence of rotational Raman scattering: molecules in the atmosphere do not absorb photons in a purely elastic (Rayleigh scattering) fashion. A small portion of the light–matter interaction is in fact inelastic [2, 18]. This changes the light source frequencies as seen from the detector. This phenomenon was first noticed by Grainger and Ring in 1962. At the time, they noticed that the well-known Fraunhofer lines would slightly change when one observed them by using moonlight instead of scattered daylight [10].

From the occurrence of these phenomena, it results that the mathematical procedure for DOAS measurements consists in solving a linear and a non-linear problem. The linear problem is solved by writing Eq. (3.17) in its matrix form:

$$\tau = \mathbf{A} \cdot X. \tag{3.18}$$

$\mathbf{A}$ is an $m \times n$ matrix, with its columns being the differential cross sections $\sigma_i{}'(\lambda)$ and the wavelength powers taking the polynomial $P(\lambda) = \sum_{j=0}^{m} a_j \cdot \lambda^j$ into account. Since the number of lines in A is much larger than the number of columns, the system is overdetermined and, in this case, we must use methods to numerically approximate a solution. It is common to use the least-squares approach, in which the best solution is the one that minimises $\chi^2 = [\tau - A \cdot X] \cdot [\tau - A \cdot X]^T$.

While the Ring effect is treated as a pseudo-absorber, a synthetically produced [4] cross section that is fitted just like any other absorber, non-linearities are addressed by applying Levenberg–Marquardt's approach to non-linear fitting problems to Eq. (3.19) [1, 18]:

$$\ln\left(\frac{I_{\text{ref}}(\lambda)}{I(\lambda + \text{shift}) + \text{offset}}\right) = \sum_{i=1}^{n} \sigma_i{}'(\lambda) \cdot \Delta\text{SC}_i + \sum_{j=0}^{m} a_j \cdot \lambda^j, \tag{3.19}$$

where shift and offset, which represent spectral wavelength shifts and stray light offsets, respectively, are responsible for the non-linear character of the problem.

3.4 DOAS tomography

As mentioned in Section 3.3, DOAS is an atmospheric analysis technique based on absorption spectroscopy, which is able to quantify several trace gases. The technique yields Slant Column Densities (SCD) for each gas, which essentially correspond to line integrals of the absorption of each target species. Hence, it is possible to acquire a number of these measurements, from different angles, and with them run one of the algorithms presented in Section 3.2 to reconstruct an image, which will be equivalent to a map of the target components concentrations.

DOAS tomography is a relatively new field of study, with the first experiments being made in the beginning of the current century, namely in Germany, with the BAB-II campaign [16, 21]. In this studies, a Long Path DOAS (active DOAS) setup was built using two telescopes and two retroreflector arrays positioned onto two towers that were constructed alongside the A656 motorway, between Heidelberg and Mannheim. These researchers used a SART approach to reconstruct the image from the acquired 16 projections. Their findings were in agreement with the mathematical models of the time [21].

More recently, Stutz and his team have built and used a similar setup to study the atmospheric profiles of aromatic hydrocarbons near an refinery plant, in Texas [22]. Their system was composed of a dual-light emitting diode light source, a telescope which acted as emitter and receiver of light and retroreflector arrays, positioned strategically in the geographic region that was being studied. The study was conducted at the same time as another, which tried to make the same analysis using in-situ monitoring [19]. At the time, both studies were shown to be in agreement, validating the tomographic system.

3.4.0.1 Long-Path DOAS Tomography applications

3.4.0.2 Passive DOAS tomography for volcanic plume studies

Chapter 4

Research Methodology

4.1 Aimed contribution

This work aims to answer its main RQ by following and pursuing the proposed hypothesis (see Section 2.3). In doing so, I will contribute with a commercially viable (from a technical perspective) atmospheric monitoring system based on DOAS, capable of not only measuring pollutant contamination but also mapping their concentration in a given geographic region. This will generate several intermediate steps, which are themselves smaller contributions:

The first intermediate step will be the development of a tomographic strategy. This will of course include the selection of a sampling geometry (consider the ones presented in Section 3.2), but also the positioning of "sources and sensors" within the selected geometry. Since the system is designed to be a passive DOAS device (see Section 3.3), careful consideration must be taken in this respect. Spectral acquisition must be done in a way that allows tomographic reconstruction, but also respecting limitations and particularities that come from working with solar light. This step corresponds to answering the first secondary Research Question (see Table 2.2).

The next step will be to write a simulation tool for the tomographic procedure. The idea is for this tool to encompass the acquisition strategy that was defined in the previous step, in order to replicate the whole measurement process and then perform the reconstruction using one or more algorithms. The simulation tool has several functions. For one, it allows the fine-tuning of the approaches without having to expend any resources in purchasing material. Besides this, it also gives gives researchers the chance to experiment with different algorithms. The routine will be divided into two modules. The first module computes the projections for a given phantom, and the second performs the reconstruction with the projection data. The point is that one can write a tomographic reconstruction routine and plug it to the projection computation module, without any interference from one to the other.

Finally we reach the instrumentation definition phase. In this stage, I will have to select the optical components necessary to build this system, including telescope,

spectrometer and all the connection components. In order to maintain this system as small as possible, I will try to avoid using optical fibers, thus minimizing energy loss between telescope and spectrometer. In this stage, I will also have to design a mechanical support that allows a drone to be equipped with the optical system, respecting all positioning and pointing requirements that such a device must entail.

4.2 Detailed work plan and scheduling

In this section, I will present the work plan that was defined and is being followed while conducting the work of the proposed thesis.I will start by Figure 4.1, a low resolution Gantt chart. This chart is comprised of the more high level tasks, which coarsely follow the previously detailed approaches and contribution goals (see 4.1 and 2.3). We can see that there are two main milestones, which correspond to the publication moments. The first of these milestones was reached in 2017, with the publication of [23].

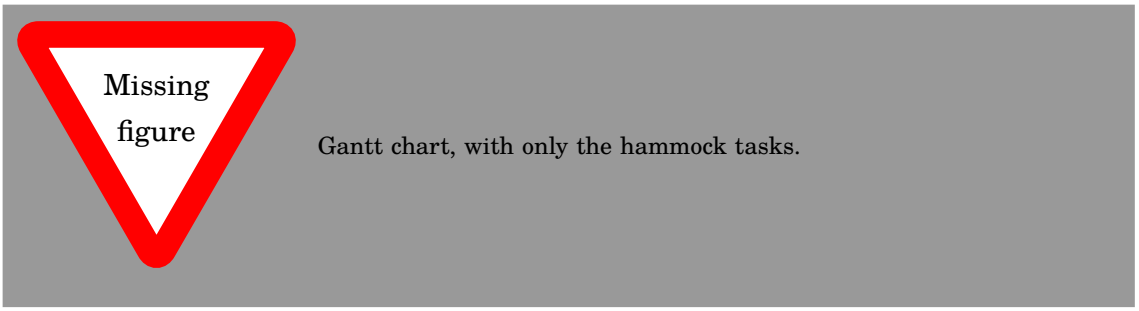

Figure 4.1: Low resolution Gantt chart for the present thesis.

Figure 4.2, Figure 4.3, Figure 4.4 and Figure 4.5 are the same Gantt chart presented in Figure 4.1, but they are *zoomed in* to each task of the project.

Figure 4.2: Zoomed Gantt chart for task 1 - ....

4.3 Validation methodology

There are several ways to validate a piece of work as the one I present here. It is important to do this in more than one, to ensure not only the validity of the project, but also its relevancy.

Figure 4.3: Zoomed Gantt chart for task 1 - ....

Figure 4.4: Zoomed Gantt chart for task 1 - ....

Figure 4.5: Zoomed Gantt chart for task 1 - ....

Before going any further, I should mention that although my project was conducted as part of the pursuit of a doctoral degree, it was not a traditional PhD, in the sense that it was not done solely in a University setting. The grant that I was awarded by the Portuguese Foundation for Science and Technology was part of a PhD Program for degrees conducted in partnership between FCT NOVA and a group of companies, named NOVA Instrumentation for Health (NOVA I4H). This is relevant as it indicates that there is at least a commercial interest in developing the technology I propose with this thesis (a market validation of sorts). Otherwise, the project would not be viable for the company.

One important way in which I will validate this project is by publishing in significant peer reviewed publications. As illustrated in Figure 4.1, during the course of my PhD, I intend to publish two relevant articles in Web-of-Science-indexed publications. The first of these was published in 2017, at the end of the preliminary studies stage

of the project. The second is currently in the finishing stages of writing and should be submitted before the end of September. Conference-wise, I plan to introduce my work to the scientific community in 2020, by participating in at least one acknowledged conference in the remote sensing or atmospheric monitoring community. Table 4.1 summarizes the project's dissemination plan.

Table 4.1: Dissemination plan for the PhD Project.

4.4 Integration with other research activities

As stated in Chapter 1, this project started as a direct evolution from the Forest Fire Finder system, an autonomous forest fire detection device. In 2017, NGNS-IS (the birthplace of FFF) was absorber by the Compta group, and FFF became Bee2Fire. As an extension to the Bee2Fire, this project is integrated in Compta's research efforts, namely in the remote sensing and artificial intelligence department.

In addition to this, the present work is supported by the Portuguese Foundation for Science and Technology, through the NOVA I4H PhD Program (grant reference: PDE/BDE/114549/2016).

Bibliography

[1] P. R. Bevington and D. K. Robinson. *Data Reduction and Error Analysis for the Physical Sciences*. 2003. ISBN: 0-07-247227-8.

[2] R. T. Brinkmann. "Rotational Raman scattering in planetary atmospheres." In: *Astrophys J* 154 (1968), pp. 1087–1093. ISSN: 0004-637X. DOI: 10.1086/149827.

[3] P. P. Bruyant. "Analytic and iterative reconstruction algorithms in SPECT." In: *Journal of nuclear medicine : official publication, Society of Nuclear Medicine* 43.10 (2002), pp. 1343–58. ISSN: 0161-5505. URL: http://jnm.snmjournals.org/cgi/content/abstract/43/10/1343%7B%5C%%7D5Cnhttp://jnm.snmjournals.org/cgi/content/full/43/10/1343%7B%5C%%7D5Cnhttp://www.ncbi.nlm.nih.gov/pubmed/12368373.

[4] K. V. Chance and R. J. D. Spurr. "Ring effect studies: Rayleigh scattering, including molecular parameters for rotational Raman scattering, and the Fraunhofer spectrum." In: *Applied Optics* 36.21 (July 1997), p. 5224. ISSN: 0003-6935. DOI: 10.1364/AO.36.005224. URL: https://www.osapublishing.org/abstract.cfm?URI=ao-36-21-5224.

[5] T. Danckaert, C. Fayt, M. Van Roozendael, I. de Smedt, V. Letocart, A. Merlaud, and G. Pinardi. *QDOAS*. 2015. URL: http://uv-vis.aeronomie.be/software/QDOAS/.

[6] M. Defrise, P. E. Kinahan, and C. J. Michel. "4 Image Reconstruction Algorithms in PET * 2D Data Organization." In: (2003), pp. 91–114.

[7] EEA. *Air pollution in Europe 1990–2004*. Tech. rep. 2. 2007.

[8] EEA. *Air quality in Europe*. Tech. rep. 28. 2016, p. 83. DOI: doi:10.2800/413142.

[9] A. Ghorani-Azam, B. Riahi-Zanjani, and M. Balali-Mood. "Effects of air pollution on human health and practical measures for prevention in Iran." In: *Journal of Research in Medical Sciences* 21.1 (2016), p. 65. ISSN: 1735-1995. DOI: 10.

4103/1735-1995.189646. URL: http://www.jmsjournal.net/text.asp?2016/21/1/65/189646.

[10] J. F. GRAINGER and J. RING. "Anomalous Fraunhofer Line Profiles." In: *Nature* 193.4817 (Feb. 1962), pp. 762–762. ISSN: 0028-0836. DOI: 10.1038/193762a0. URL: http://www.nature.com/doifinder/10.1038/193762a0.

[11] R. Gunderman. *Essential Radiology: Clinical Presentation, Pathophysiology, Imaging, 2nd ed.* 2nd ed. Thieme, 2006. ISBN: 9781588900821.

[12] G. T. Herman. "Image Reconstruction From Projections." In: *Real-Time Imaging* 1.1 (1995), pp. 3–18. ISSN: 10772014. DOI: 10.1006/rtim.1995.1002.

[13] G. T. Herman. *Fundamentals of Computerized Tomography*. Advances in Pattern Recognition. London: Springer London, 2009. ISBN: 978-1-85233-617-2. DOI: 10.1007/978-1-84628-723-7. URL: http://link.springer.com/10.1007/978-1-84628-723-7.

[14] G. T. Herman, A. Lent, and S. W. Rowland. "ART: Mathematics and applications. A report on the mathematical foundations and on the applicability to real data of the algebraic reconstruction techniques." In: *Journal of Theoretical Biology* 42.1 (1973). ISSN: 10958541. DOI: 10.1016/0022-5193(73)90145-8.

[15] A. C. Kak. "Algebraic Reconstruction Algorithms." In: *Computerized Tomographic Imaging*. 2001, pp. 275–296. ISBN: 978-0-89871-494-4. DOI: 10.1137/1.9780898719277.ch7.

[16] T. Laepple, V. Knab, K.-U. Mettendorf, and I. Pundt. "Longpath DOAS tomography on a motorway exhaust gas plume: numerical studies and application to data from the BAB II campaign." In: *Atmospheric Chemistry and Physics Discussions* 4.3 (2004), pp. 2435–2484. ISSN: 1680-7375. DOI: 10.5194/acpd-4-2435-2004. URL: http://www.atmos-chem-phys-discuss.net/4/2435/2004/.

[17] G. M. Lovett, T. H. Tear, D. C. Evers, S. E. Findlay, B. J. Cosby, J. K. Dunscomb, C. T. Driscoll, and K. C. Weathers. "Effects of Air Pollution on Ecosystems and Biological Diversity in the Eastern United States." In: *Annals of the New York Academy of Sciences* 1162.1 (Apr. 2009), pp. 99–135. ISSN: 00778923. DOI: 10.1111/j.1749-6632.2009.04153.x. URL: http://doi.wiley.com/10.1111/j.1749-6632.2009.04153.x.

[18] A. Merlaud. *Development and use of compact instruments for tropospheric investigations based on optical spectroscopy from mobile platforms*. Louvain: Presses Universitaires de Louvain, 2013. ISBN: 978-2-87558-128-0. URL: http://books.google.com/books?hl=en%7B%5C&%7Dlr=%7B%5C&%7Did=inXVSyR82zwC%7B%5C&%7Doi=fnd%7B%5C&%7Dpg=PR3%7B%5C&%7Ddq=Development+and+use+of+compact+instruments+for+tropospheric+investigations+based+on+optical+spectroscopy+from+mobile+platforms+sciences%7B%5C&%7Dots=VdebeDBQMc%7B%5C&%7Dsig=4G0eVEvthJXuqd8WI3IWjjVXuXc.

[19] E. P. Olaguer. “Overview of the Benzene and Other Toxics Exposure (BEE-TEX) Field Study.” In: *Environmental Health Insights* 9s4 (Jan. 2015), EHI.S15654. ISSN: 1178-6302. DOI: 10.4137/EHI.S15654. URL: http://journals.sagepub.com/doi/10.4137/EHI.S15654.

[20] U. Platt and J. Stutz. *Differential Optical Absorption Spectroscopy*. Heidelberg, Germany: Springer, 2007. ISBN: 9783540211938.

[21] I. Pundt, K. U. Mettendorf, T. Laepple, V. Knab, P. Xie, J. Lösch, C. V. Friedeburg, U. Platt, and T. Wagner. “Measurements of trace gas distributions using Long-path DOAS-Tomography during the motorway campaign BAB II: Experimental setup and results for NO 2.” In: *Atmospheric Environment* 39.5 (2005), pp. 967–975. ISSN: 13522310. DOI: 10.1016/j.atmosenv.2004.07.035.

[22] J. Stutz, S. C. Hurlock, S. F. Colosimo, C. Tsai, R. Cheung, J. Festa, O. Pikelnaya, S. Alvarez, J. H. Flynn, M. H. Erickson, and E. P. Olaguer. “A novel dual-LED based long-path DOAS instrument for the measurement of aromatic hydrocarbons.” In: *Atmospheric Environment* 147 (Dec. 2016), pp. 121–132. ISSN: 13522310. DOI: 10.1016/j.atmosenv.2016.09.054. URL: http://linkinghub.elsevier.com/retrieve/pii/S1352231016307713.

[23] R. Valente de Almeida and P. Vieira. “Forest Fire Finder – DOAS application to long-range forest fire detection.” In: *Atmospheric Measurement Techniques* 10.6 (June 2017), pp. 2299–2311. ISSN: 1867-8548. DOI: 10.5194/amt-10-2299-2017. URL: https://www.atmos-meas-tech.net/10/2299/2017/.

[24] P. Vieira and J. Matos. *SYSTEM FOR AUTOMATIC DETECTION OF FOREST FIRES THROUGHOPTC SPECTROSCOPY*. 2008.

[25] P. Vieira, J. Matos, and M. Mendes. *Sistema para a detecção automática de incêndios florestais por espectroscopia óptica*. 2007.

[26] World Health Organisation Europe. “Health Aspects of Air Pollution Results from the WHO Project "Systematic Review of Health Aspects of Air Pollution in Europe".” In: *World Health* (2004), p. 30.